



ELSEVIER

1 December 1996

**OPTICS
COMMUNICATIONS**

Optics Communications 132 (1996) 295–301

Development of a sliding discharge pumped HF laser

G.N. Tsikrikas, A.A. Serafetinides, A.D. Papayannis

National Technical University of Athens, Physics Department, Zografou Campus, Athens 15780, Greece

Received 25 January 1996; accepted 24 April 1996

Abstract

Direct excitation by a surface sliding discharge is applied for the first time to an HF laser. The laser operates at atmospheric pressure with a gas mixture of He/SF₆/C₃H₈. Details are presented on the efficiency of energy transfer, the dependence of laser performance on input energy deposition, circuit parameters and gas mixture. The F atom production rate is estimated from the linear dependence of the specific output energy on the electric charge passed through the discharge. Output energies of 135 mJ were obtained at 1.2% efficiency from a small active discharge of 10 cm³ volume and 38 cm length. These values compare favourably with the values reported for similar laser systems, while the maximum values of specific input and output energy extraction obtained, of 1700 and 15 J/l respectively, are among the highest reported for non-chain-reaction type gas mixtures. These results demonstrate that the sliding discharge, although simple in design, is an efficient scheme for developing gas discharge lasers.

PACS: 42.55.E, 42.60.B

1. Introduction

Pulsed HF lasers were developed extensively [1] in the 1970s and the beginning of the 1980s for their ability of producing very high output energy levels. The recent interest for laser sources in the wavelength region of 3 μm for medical applications [2], revived the interest in compact, easy to handle HF lasers, which, together with the Er:YAG laser are the only laser sources in this region.

Sliding or corona discharges are commonly used as preionisers in gas lasers [3]. They have also been used as plasma electrodes [4] in CO₂, excimer, N₂ and recently in the HF laser as well [5]. Additionally, sliding discharges have been used for direct laser pumping of N₂ [6], Ar, Xe [7], Ne [8] and XeF [9] lasers.

Here we report the operation of an HF laser pumped by the discharge along the surface of a dielectric. The sliding discharge scheme has been used in the past for excitation of the HF laser, but in the photo-initiation mode, in which the UV radiation is emitted by the sliding discharge, was used to photo-initiate the chain reaction in an (F₂,H₂) type laser mixture [10,11]. In Ref. [10], the sliding discharge was a uniform plasma sheet covering the inner surface of the cylindrical laser head, while in Ref. [11] it had the form of a single long spark channel. Photo-initiation has also been used in the XeF laser [9]. Excitation by the sliding discharge itself is, to the best of our knowledge, applied for the first time to an HF laser.

The sliding discharge exhibits some unique properties which distinguish it from other discharge types.

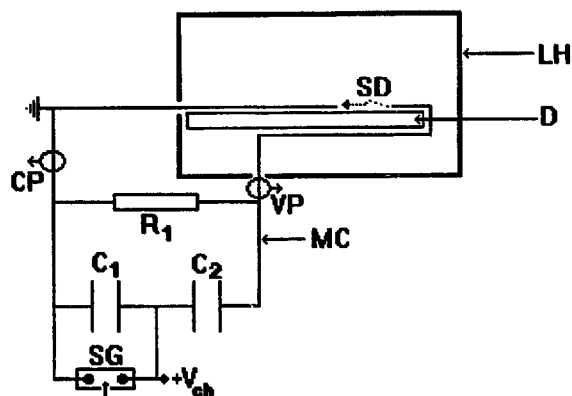


Fig. 1. Electrical driving circuit scheme and laser head arrangement. C_1 , C_2 capacitors, R charging resistor, SG spark gap switch, V_{ch} charging voltage, CP and VP current and voltage probes respectively, A metal anode, SD sliding discharge, D dielectric plate, LH plexiglas laser chamber and MC copper or aluminium foil metal connections.

In the configuration most commonly used, one of the electrodes continues on the back side of the dielectric (Fig. 1). The application of a sufficiently fast high voltage pulse (rate of rise $\geq 10^{11}$ V/s), leads to the production of a plasma sheet adjacent to the surface of the dielectric. The presence of the conductive back-plane allows the formation of a distributed capacitance in the dielectric and also reduces the system inductance. The sliding discharge uniformity increases with increasing specific capacitance of the dielectric, since the latter controls the number density of the displacement type current channels which are capacitively distributed along the electrode length. Also, due to the presence of the substrate electrode, the application of an electric field polarises the dielectric and creates surface charges which in turn leads to the generation of a strong electric field component perpendicular to the dielectric surface. High electric field values and hence large amounts of high energy electrons and of UV radiation can be produced with moderate values of applied voltage, due to (i) the strengthening of the total field by the presence of the normal field component, (ii) additional field intensity enhancements on the micro-irregularities of the surface, and (iii) the confinement of the discharge on the dielectric surface. The UV radiation is additionally enhanced by the emission from species adsorbed from the dielectric surface and also from ablated dielectric constituents which

are incorporated into the discharge [4,12]. Thus, the ease of obtaining uniform, high current sliding surface discharges and the presence of strong electric fields, makes them attractive for direct laser excitation, especially for media which require high electron energies for their optimum pumping.

2. Laser description

The dielectric used for the formation of the sliding discharge was standard epoxy-fiber-glass circuit board with a dielectric constant in the region $\epsilon = 3-5$ and thickness of $\Delta = 0.8$ mm. The specific capacitance of the dielectric is $C_{sp} = 0.88 \epsilon / \Delta$ (in pF/cm²) where Δ is in mm [12], which gives $C_{sp} = 3-6$ pF/cm². Initially, the sliding discharge electrodes were produced by directly etching the copper layer on the surface of the circuit board. However, due to the very small thickness of the copper layer, the electrodes were easily destroyed by the discharge and also it was difficult to obtain high quality electrode profiles with the etching procedure. Hence, aluminium electrodes of 38 cm active length and 1 mm thickness with an Ernst type profile were built instead. The profile parameters were chosen so as to give a uniform electric field for the 38 cm active electrode length. Laser performance was critically dependent on the electrode profile. The use of the uniform field electrodes resulted in more than 50% increase in the arc free discharge input energy loading. The electrodes were held in pressure contact with the surface of the dielectric. The electrode structure was contained in a plexiglas chamber of dimensions $50 \times 14 \times 10$ cm³, with the mirrors attached directly on its sides. The resonator was formed by a 10 m radius of curvature gold coated copper mirror and a plane CaF₂ output coupler.

The gas mixture was He/SF₆/C₃H₈, with typical flow ratios 10/0.2/0.02 l/min, at an overall atmospheric pressure. This gas mixture with inert F and H donors eliminates any difficulties and inconveniences caused by the highly efficient but very corrosive and explosive neat F₂ and H₂ respectively. As in most conventional design chemical lasers, the operational frequency was limited by the gas flow rate to 1 Hz. It was decided to work at atmospheric

pressure in order to obtain a device as simple and compact as possible.

The electrical driving circuit is shown in Fig. 1. The sliding discharge was driven by an *LC* inversion type circuit (capacitors C_1 , C_2). The capacitors used had nominal values of 2 nF, 40 kV. Special care was taken to minimise the inductance of the circuit. The two feed-through electrical connections of the laser chamber (Fig. 1) were continuous along the length of the electrodes. The spark gap had a self-inductance of 15 nH. The inductance of the inversion circuit main loop was $L_m = 30\text{--}40$ nH depending on the circuit capacitance and the corresponding value for the switching loop was $L_s = 35\text{--}40$ nH. These values were calculated from the self ringing frequency of the corresponding loops under short-circuiting of the electrode gap [12] and also by using the well known solenoid approximation formula $L = \mu_0 N^2 A / l$, with $N = 1$, where A and l are the cross-sectional area and length of the current sheet respectively [13].

3. Laser performance

The dependence of laser performance on discharge input energy loading was investigated for different values of charging voltage V_{ch} , total capacitance C ($C_1 = C_2 = C/2$) and electrode gap g . The charging voltage was limited to 28.5 kV by the available power supply. Results were obtained for

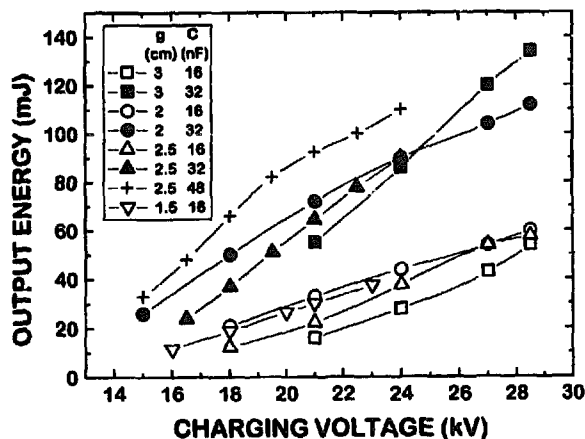


Fig. 2. Output energy E_{out} as a function of charging voltage, for different values of circuit capacitance C and electrode gap g .

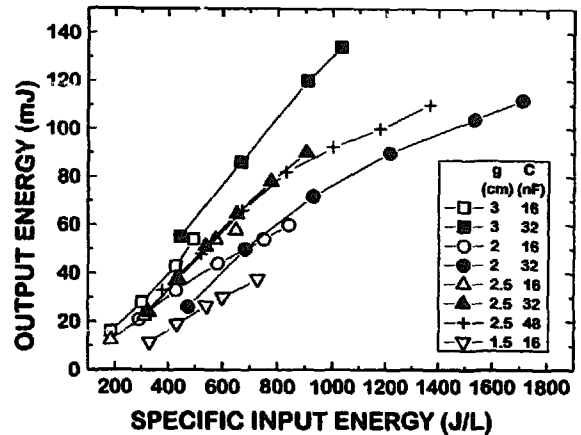


Fig. 3. Output energy E_{out} as a function of specific input energy, for different values of circuit capacitance C and electrode gap g .

$C = 16, 32$ and 48 nF and $g = 1.5, 2.0, 2.5$ and 3.0 cm.

In Fig. 2 the dependence of output energy E_{out} on charging voltage V_{ch} is shown. In Figs. 3 and 4 the dependence of respectively the output energy and efficiency η on specific input energy is shown. For the larger values of capacitance $C = 32$ and 48 nF, maximum efficiency is obtained at specific input energy in the range $E_{in} = 800\text{--}1000$ J/l which seems to be the optimum pumping regime. For the lower value of capacitance $C = 16$ nF, maximum efficiency is obtained at E_{in} values in the range $400\text{--}600$ J/l. The discharge width was measured to be 1 mm as expected from the confined nature of the sliding

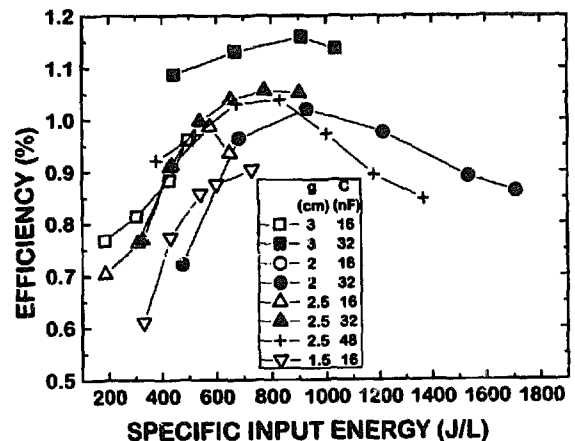


Fig. 4. Efficiency η as a function of specific input energy, for different values of circuit capacitance C and electrode gap g .

discharge and thus the active discharge volume varied from 5.7 to 11.4 cm³ for the range of electrode gap values tried.

The maximum output energy and efficiency were obtained for $C = 32$ nF and $g = 3$ cm. The maximum output energy was $E_{\text{out}} = 134$ mJ at $\eta = 1.14\%$ efficiency at the maximum available charging voltage of 28.5 kV while the maximum efficiency was $\eta = 1.16\%$ at $E_{\text{out}} = 120$ mJ. The corresponding specific input and output energies were 910 and 10.5 J/l respectively. The maximum values of specific input and output energies were 1700 and 15 J/l respectively and were obtained for $C = 32$ nF and $g = 2$ cm at a reduced efficiency of $n = 0.86\%$ and $E_{\text{out}} = 112$ mJ.

The factors that affect laser performance are better understood by separating the laser efficiency η into two main contributions, (a) the efficiency of energy transfer η_{tr} from the driving circuit to the discharge, $\eta_{\text{tr}} = E_{\text{d}}/E_{\text{in}}$, where E_{d} is the deposited energy as defined in Eq. (1) and E_{in} is the stored energy, and (b) the intrinsic laser efficiency η_{int} defined as the ratio of the laser output energy to the deposited energy, $\eta_{\text{int}} = E_{\text{out}}/E_{\text{d}}$. The efficiency η_{tr} is related to the matching of the discharge impedance with that of the driving circuit. For the calculation of the discharge resistance R we used an average value R_{av} , as defined in Ref. [13], which is more realistic than the commonly used value at peak current:

$$R = R_{\text{av}} = E_{\text{d}} / \int_0^{\tau} I_{\text{d}}^2 dt, \quad (1)$$

where

$$E_{\text{d}} = \int_0^{\tau} V_{\text{d}} I_{\text{d}} dt$$

is the energy deposited in the main discharge, and V_{d} , I_{d} are the sliding discharge voltage and current respectively. The damping constant ρ has its usual definition as

$$\rho = R_{\text{av}} / \rho_{\text{c}}, \quad (2)$$

where

$$\rho_{\text{c}} = 2(L_{\text{e}}/C_{\text{e}})^{1/2}$$

is the resistance for critical damping. The L_{e} and C_{e} are the 'effective' inductance and capacitance values for the LC inversion main loop and R_{av} was defined in Eq. (1).

A study was made for the factors that affect η_{tr} and η_{int} for two values of discharge gap and capacitance, $g = 2$ and 3 cm and $C = 16$ and 32 nF. In all cases the discharge resistance R_{av} decreases with charging voltage. However for $g = 2$ cm, $R_{\text{av}} < \rho_{\text{c}}$ and thus $\rho < 1$ while for $g = 3$ cm, $R_{\text{av}} > \rho_{\text{c}}$ and thus $\rho > 1$. As a consequence η_{tr} decreases with charging voltage for $g = 2$ cm and increases for $g = 3$ cm respectively.

For a fixed value of specific input energy and capacitance, the output energy and efficiency increase as the electrode gap is increased. This is mainly attributed to the increase in the discharge resistance R with electrode gap and the corresponding improvement of the energy transfer efficiency η_{tr} . For instance, for $E_{\text{in}} = 920$ J/l and $C = 32$ nF the corresponding values of R and η_{tr} increased from $R = 4$ to 6.3 Ω and from $\eta_{\text{tr}} = 52\%$ to 57% respectively, as the electrode gap increased from 2 to 3 cm. Thus, for a given range of charging voltage, one can select the appropriate value of electrode gap that maximises η_{tr} . The optimum value, in our case, seems to be around $g = 4$ cm. However, the laser head construction permitted the use of electrode gap values up to $g = 3$ cm. The maximum η_{tr} was at $\eta_{\text{tr}} = 57\%$, obtained for $g = 3$ cm and $C = 32$ nF for $V_{\text{ch}} = 28.5$ kV.

The internal efficiency η_{int} as well as the steady state electric field E_{ss} , i.e. the field value at peak current, were found to be practically independent of charging voltage, electrode gap and capacitance. For all the parameter values tried, η_{int} varied between 1.8% and 2.0% and E_{ss} between 8.95 and 9.73 kV/cm, the corresponding relative changes being 12% and 8% respectively. The η_{int} reflects the efficiency of the laser pumping process which can be traced back to the efficiency of F atom production by the dissociation of SF₆ molecules by electron impact. Since the discharge remains in a quasi-steady phase, for a time period of 30–60 ns, during which the electric field equals E_{ss} and most of the energy is deposited in the discharge, all field dependent processes and thus F atom production can be considered to occur at a constant rate and this results in a constant internal efficiency. Since E_{ss} depends to a first approximation only on gas mixture composition, the same holds for η_{int} as well.

The discharge impedance increases as the SF₆

concentration gets larger. The average discharge resistance R_{av} increases from 2.6 to 3.9 Ω as the SF_6 content increases from 1.3% to 4.3%. The maximum values of η_{tr} and η_{int} were obtained for an SF_6 concentration of 2.2%.

It should be noted that the performance of the sliding discharge is critically dependent on the polarity of the applied voltage pulse. Experiments showed that the sliding discharge was less intense but more uniform when the polarity of the electrode that continues on the back-plane of the dielectric was negative. The laser output energy was up to two times higher than in the case of positive polarity. A complete investigation of the polarity influence on the laser performance will be presented in a separate article.

The dependence of the output energy on the SF_6 concentration in percentage in the gas mixture for a constant ratio γ of SF_6 to C_3H_8 partial pressures at $\gamma = 11$ is shown in Fig. 5, as well as the dependence of E_{out} on the ratio γ of SF_6 to C_3H_8 partial pressures, for a constant SF_6 concentration of 2.2%. The dependence on γ is more critical than that on the SF_6 content. The maximum energy is obtained for a value $\gamma = 11$. The dependence of peak discharge voltage V_{pk} , voltage at peak current V_{ss} (steady state voltage) and peak discharge current I_{pk} , on the

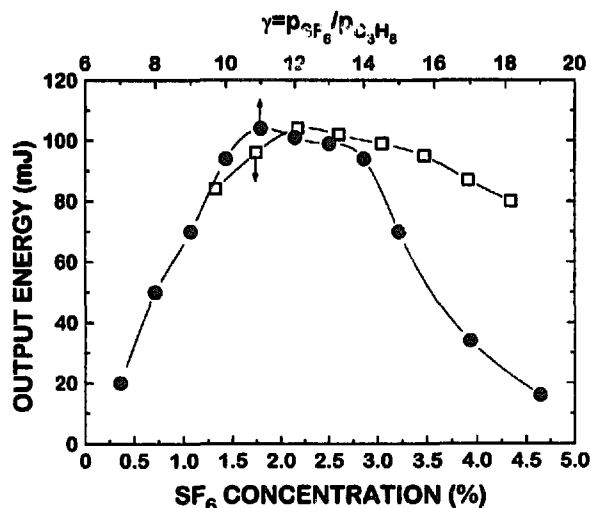


Fig. 5. Output energy E_{out} , as a function of the SF_6 concentration in percentage for a constant value of $\gamma = 11$ and also as a function of the ratio γ of SF_6 to C_3H_8 partial pressures, for a constant SF_6 concentration of 2.2%.

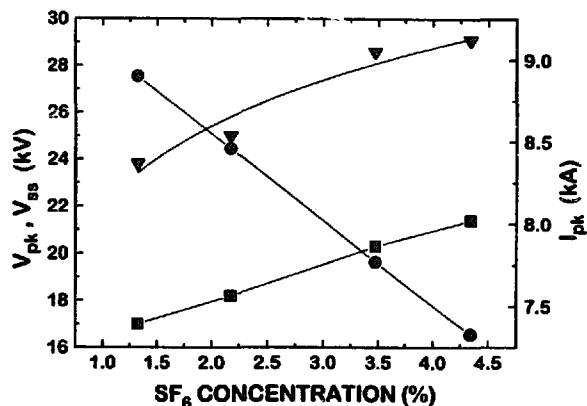


Fig. 6. Dependence of the discharge, peak voltage V_{pk} (triangles), voltage at peak current or steady state voltage V_{ss} (squares) and peak current I_{pk} (circles), on the SF_6 concentration in percentage.

SF_6 concentration is shown in Fig. 6. A similar behaviour is also obtained as the C_3H_8 content is increased. A larger content of SF_6 results in a larger production of F atoms and hence of laser output, since more SF_6 donor molecules are present. On the other hand, due to the strong attaching property of SF_6 , the breakdown and steady state discharge voltage increase with SF_6 content while the peak discharge current is reduced. The steady state field E_{ss} increased from 8.5 to 10.7 kV/cm for an increase in the SF_6 content from 1.3% to 4.3%. The optimum concentration is obtained from the balance between the steady state electric field value which gives the maximum F production rate and the decreasing amount of current that is passing through the discharge as the SF_6 concentration is increased. As the charging voltage V_{ch} is increased, a larger SF_6 concentration is required in order to sustain the optimum value of V_{ss} and hence to obtain maximum output. The reduced output at lower C_3H_8 concentrations (higher γ) is explained qualitatively because there is insufficient C_3H_8 to balance the F production rate, whereas at lower values of γ the output is reduced due to an increased rate of vibrational relaxation of HF(v) molecules by C_3H_8 and also by the increasing amount of electron energy that is lost in ionising and dissociating the C_3H_8 molecules.

The current and voltage waveforms for the sliding discharge (I_d , V_d), as well as the laser output pulse, are shown in Fig. 7 for $V_{ch} = 27$ kV, $C = 32$ nF and

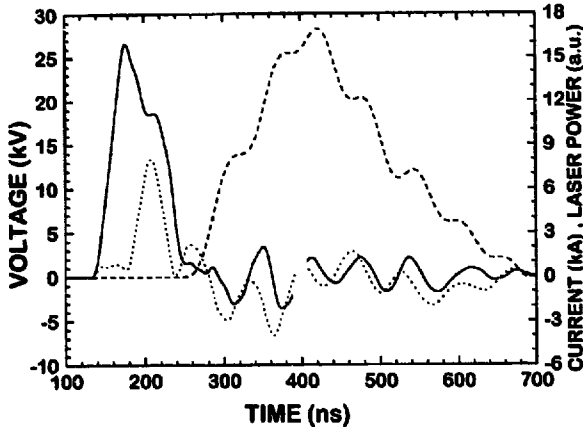


Fig. 7. Current I_d (short dash) and voltage V_d (solid) waveforms for the sliding discharge and the laser output pulse power (long dash).

$g = 2$ cm. The waveforms were recorded on a digital oscilloscope (HP-5430A) and stored for later processing. The voltage waveforms were measured with a Tektronics P6015 high voltage probe, the current with a self-made Rogowski coil, while the laser output power was monitored with a Laser Probe KT-1510 fast pyroelectric detector. The position of the probes is shown in Fig. 1. Only a small part of the total current was passed through the coil to keep the inductance increase to a minimum. The current probe was calibrated using the method described in Ref. [13], i.e. by calculating the charge transferred from the capacitors to the discharge during the current pulse and equating it with that obtained from the integration of the observed current waveform. The V_d was obtained from the observed voltage waveform after subtracting the inductive part $L_h dI_d/dt$, where L_h is the inductance between the insertion point of the voltage probe and the discharge electrodes. The value of L_h was estimated using the solenoid formula (section 2) to be $L_h = 15$ nH. At the end of the current pulse, except for the case of high specific energy loading, there was a finite voltage remaining on the main discharge electrodes due to the strong electron attachment of SF_6 . For instance for the case of $C = 32$ nF and $g = 3$ cm, the remaining voltage ranged from 16 to 12 kV for a corresponding charging voltage range from 21 to 28.5 kV. The energy left on the capacitors was subtracted in the calculation of input energy. Typical values for the rise time

of the discharge voltage were $t_r = 30$ – 50 ns and for the rate of increase 7×10^{11} V/s, the corresponding current values being 20–30 ns and 3×10^{11} A/s respectively. The V_d remained at its steady state value V_{ss} for approximately 30–60 ns and then collapsed to the final value. The current flow during the voltage rise time is due to the charging of the distributed capacitance of the dielectric. Using the formula $i = C_{sd} dV/dt$ the distributed capacitance was found to be $C_{sd} = 0.8$ – 1.0 nF which is larger than the value obtained from the calculation in section 2 which gives for $g = 2$ cm, $C_{sd} = 0.2$ – 0.4 nF. This discrepancy may be due to the presence of parasitic capacitance in the laser head construction.

The laser output pulse had the typical form of an HF laser multipeak structure due to the cascading nature of the de-excitation process of adjacent vibrational levels. The FWHM was 170 ns and the base width 350 ns. The corresponding peak power value for the maximum output energy was $P_{pk} = 0.8$ MW. The different gas mixture concentrations and input energy values resulted in only minor changes on the peak structure and time characteristics of the laser pulse.

In Ref. [14] it was shown that the output energy of a DF laser was proportional to the electric charge that passed from the discharge and using this dependence the F production rate in the discharge was

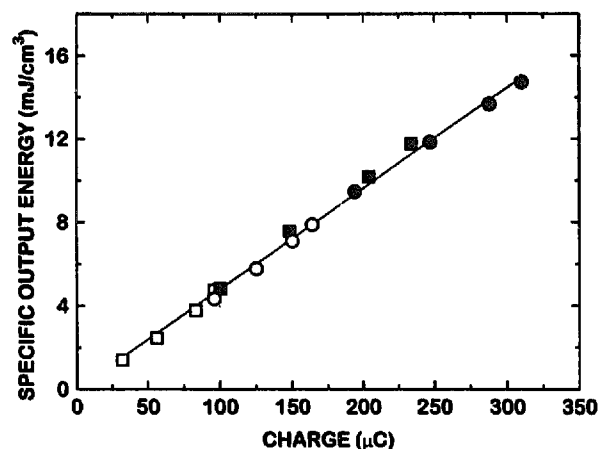


Fig. 8. Specific output energy as a function of the electric charge that passed through the discharge, for different values of capacitance, electrode gap and charging voltage (squares $g = 3$ cm, circles $g = 2$ cm, open $C = 16$ nF, filled $C = 32$ nF). The slope of the linear fit is 0.0482 mJ/(cm³ μ C).

estimated. The same linear dependence of the specific output energy on the charge Q that passed from the discharge during the main current pulse, was observed in our system and is shown in Fig. 8. The data points are for values of V_{ch} between 21 and 28.5 kV, C of 16 and 32 nF, electrode gaps of $g = 2$ and 3 cm and for an SF_6 content of 2.2%. Following the reasoning of Ref. [14], the observed dependence can be interpreted as follows. As was described above, there is a steady state phase of the discharge during which the electric field is constant or slowly varying. Moreover, this steady state field E_{ss} is independent of the circuit parameters and depends only on the gas mixture composition. Consequently, within this steady state time period, all the field dependent processes, such as the F production, can be assumed to occur at a constant rate. The slope of the linear fit in Fig. 8 is strikingly the same as the one obtained for the same calculation in the case of a completely different design HF laser, developed by our group [5], but which used the same mixture composition at the same component ratio and pressure. This result strongly supports the reasoning of the calculation proposed in Ref. [14]. The value of the F production rate was estimated to be $k_{\text{F}} = 2.2 \times 10^{-9} \text{ cm}^3/\text{s}$ under the same assumptions as in Ref. [5].

4. Conclusion

It was demonstrated that the sliding discharge design scheme can be successfully applied to the HF laser. The F production rate in the discharge was estimated to be $k_{\text{F}} = 2.2 \times 10^{-9} \text{ cm}^3/\text{s}$ from the linear dependence of the specific output energy on the charge Q that passed from the discharge during the main current pulse. On account of the small active discharge volume of 10 cm^3 and length of 38 cm and the moderate value of charging voltage (up to 28.5 kV), the value of the output energy of 134 mJ at 1.14% efficiency compares favourably with the

values reported for similar laser systems, while the maximum values of specific input and output energy extraction obtained, 1710 and 15 J/l respectively, are among the highest reported for non-chain-reaction type gas mixtures. These results demonstrate that the sliding discharge, although simple in design, is an efficient scheme for developing gas discharge lasers.

Acknowledgements

We are grateful to C. Razakias and C. Gemenetzis for their technical assistance.

References

- [1] A.V. Eletsii, *Sov. Phys. Usp.* 24 (1981) 475.
- [2] G.L. Valderrama, R.F. Menefee, B.D. Krenek and M.J. Berry, *SPIE* 1064 (1989) 135.
- [3] R.S. Taylor and K.E. Leopold, *Rev. Sci. Instrum.* 65 (1994) 3621.
- [4] D.Yu. Zaruslov, G.P. Kuz'min and V.F. Tarasenko, *Radio Eng. Electr. Phys.* 29 (1984) 1.
- [5] G.N. Tsirikas, A.A. Serafetinides and A.D. Papayannis, *Appl. Phys. B* 62 (1996) 357.
- [6] P.P. Branzalov, B.O. Zikrin, N.V. Karlov, I.O. Kovalev, A.V. Korablev, G.P. Kuz'min and V.F. Perov, *Sov. Tech. Phys. Lett.* 14 (1988) 419.
- [7] P.A. Atanasov and A.A. Serafetinides, *Optics Comm.* 72 (1989) 356.
- [8] P.A. Atanasov, S.G. Vasilev and A.A. Serafetinides, *Opt. Laser Techn.* 25 (1993) 31.
- [9] R.W.F. Gross, L.E. Schneider and S.T. Amimoto, *Appl. Phys. Lett.* 53 (1988) 2365.
- [10] V.M. Borisov, A.M. Davidovskii, S.G. Mamonov and O.B. Khristoforov, *Sov. J. Quantum Electron.* 13 (1983) 681.
- [11] H. Hokazono, K. Hishinuma, K. Watanabe, M. Obara and T. Fujioka, *J. Appl. Phys.* 53 (1982) 1359.
- [12] R.E. Beverly III, *J. Appl. Phys.* 60 (1986) 104.
- [13] H. Houtman, A. Cheuck, A.Y. Elezzabi, J.E. Ford, M. Laberge, W. Liese, J. Meyer, G.C. Stuart and Y. Zhu, *Rev. Sci. Instrum.* 64 (1993) 839.
- [14] E.K. Gorton, E.W. Parcell and P.H. Cross, *Optics Comm.* 70 (1989) 399.